J. metamorphic Geol., 1994, **12**, 455–466

Tectonic setting, petrology and geochronology of jadeite + glaucophane and chloritoid + glaucophane schists from north-west Turkey

A. I. OKAY[1] AND S. P. KELLEY[2]
[1]*ITÜ Maden Fakültesi, Jeoloji Bölümü, Ayazağa, 80626 Istanbul, Turkey*
[2]*Department of Earth Sciences, Open University, Milton Keynes MK7 6AA, UK*

ABSTRACT The north-west Turkish blueschists represent a subducted passive continental margin sequence dominated by metaclastic rocks and marble. The depositional age of the blueschist protoliths are probably Palaeozoic to Mesozoic, while the age of the high-pressure/low-temperature metamorphism is Late Cretaceous. Blueschists are tectonically overlain by a volcanosedimentary sequence made up of accreted oceanic crustal material that locally shows incipient blueschist metamorphism and by spinel peridotite slices.

The metaclastic rocks with regional jadeite and glaucophane, which comprise the lower part of the blueschist unit, make up an over 1000-m-thick coherent sequence in the Kocasu region of north-west Turkey. Rare metabasic horizons in the upper parts of the metaclastic sequence with sodic amphibole + lawsonite but no garnet indicate lawsonite blueschist facies metamorphism. The blueschist metaclastics in the Kocasu region are practically free of calcium and ferric iron and closely approximate the NFMASH system in bulk composition. Two low-variance mineral assemblages (with quartz and phengite) are jadeite + glaucophane + chlorite + paragonite and chloritoid + glaucophane + paragonite. The metaclastics comprise up to several-metres-thick layers of jadeite schist with quartz, phengite and nearly 100 mol% jadeite. Phase relations in the metaclastics show that the chloritoid + glaucophane assemblage, even in Fe^{2+}-rich compositions, is stable in the jadeite stability field. In the NFASH system the above assemblage without the accompanying garnet has a narrow thermal stability field.

Mineral equilibria in the metaclastics involving chloritoid, glaucophane, jadeite, paragonite and chlorite indicate metamorphic P–T conditions of 20 ± 2 kbar and 430 ± 30 °C, yielding geothermal gradients close to 5° C km^{-1}, one of the lowest geotherms recorded. Blueschists in the Kocasu region, which have been buried to 70 km depth, are tectonically overlain by the volcanosedimentary sequence and by peridotite buried not deeper than 30 km.

Phengites from two jadeite schists were dated by Ar/Ar laser probe; they give an age of 88.5 ± 0.5 Ma, interpreted as the age of metamorphism. Blueschists and the overlying peridotite bodies are intruded by 48–53-Ma-old granodiorite bodies that were emplaced at 10 km depth. This suggests that the exhumation of blueschists by underplating of cold continental crust, and normal faulting at the blueschist–peridotite, interface occurred during the Late Cretaceous to Palaeocene (88–53 Ma).

Key words: Ar/Ar dating; blueschist; jadeite; NFMASH system; north-west Turkey.

INTRODUCTION

Regional jadeite-bearing blueschist facies rocks are rare, requiring unusual lithologies and exceptional metamorphic conditions for their formation and preservation. The only well-known example is the Diablo Range in California, where the Franciscan metagreywackes have developed regional jadeite (e.g. McKee, 1962; Ernst, 1965; Moore & Liou, 1979). In the eclogite facies, jadeite- and garnet-bearing rocks have been described from the Sesia-Lanzo Zone in the Western Alps (Compagnoni, 1977) and in minor amounts from New Caledonia (Black *et al.*, 1988), from Sifnos Island in the Cyclades in Greece (Okrusch *et al.*, 1978; Schliestedt & Okrusch, 1988), and from the Maksyutov Complex in the southern Urals (Sobolev *et al.*, 1986). In north-west Turkey, jadeite-bearing blueschist facies rocks associated with chloritoid–glaucophane schists occur over an area of over 75 km^2 and form a coherent regional metamorphic terrane. Apart from their intrinsic interest, the compositions of the metaclastics in this region are virtually free of both calcium and ferric iron components, and they closely approximate the NFMASH system. This allows a much narrower estimate of the blueschist facies P–T conditions in this region and provides a field test for the recent NFMASH petrogenetic grids (Guiraud *et al.*, 1990; El-Shazly & Liou, 1991).

REGIONAL SETTING

Late Cretaceous blueschists form a 40-km-wide and over 250-km-long coherent metamorphic belt in north-west Turkey, south of the Tethyan Izmir–Ankara suture (Fig. 1). The suture formed as a result of northward subduction

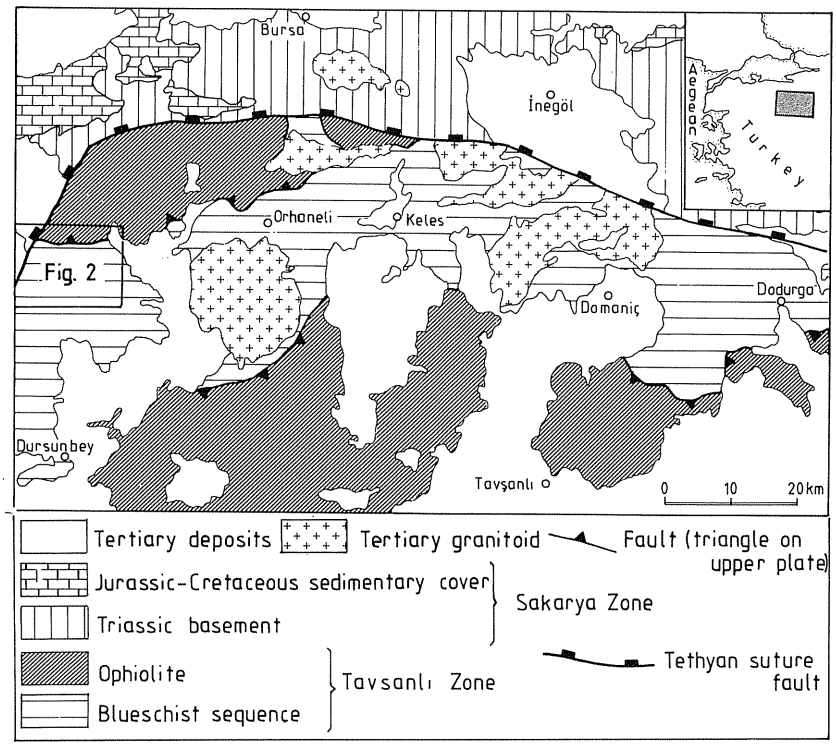

Fig. 1. Tectonic map of north-western Turkey. The study area shown in Fig. 2 is indicated.

of the Tethyan oceanic lithosphere and resulting Late Cretaceous to Early Tertiary continental collision between the active margin of the northern plate (Sakarya Zone of the Pontides) and the passive margin of the southern plate represented by the blueschist belt in north-west Turkey (Şengör & Yılmaz, 1981; Okay, 1986). The blueschist sequence consists of a lower metaclastic unit over 1000 m in thickness which passes stratigraphically upward into a marble series several thousand metres thick, which is in turn overlain by a varied sequence of metabasite, metachert and metashale (Okay, 1984, 1986). Deposition of the premetamorphic sequence was probably Palaeozoic to Mesozoic based on broad stratigraphic correlation with unmetamorphosed units further south, where the Late Palaeozoic is represented by clastic rocks and the Mesozoic by neritic carbonate rocks. Published isotopic data on the high-pressure/low-temperature metamorphism comprise two phengite K–Ar ages, of 65 and 82 Ma, from the eastern end of the blueschist belt, 250 km east of the area studied (Çoğulu & Krummenacher, 1967).

In north-west Turkey, blueschists are tectonically overlain by a disrupted volcanosedimentary sequence, which in some areas shows an incipient blueschist metamorphism with the development of lawsonite and aragonite in the amygdules of spilites and replacement of igneous augite by sodic pyroxene in spilitized basic volcanic rocks (Okay, 1982). Large peridotite bodies tectonically overlie the volcanosedimentary sequence or directly overlie the blueschists.

Blueschists, the volcanosedimentary sequence and the peridotite, which together constitute the Tavşanlı Zone, are thrust southward over a greenschist facies metasedimentary sequence. Early Tertiary granodiorites intrude the Tavşanlı Zone, and Miocene volcanic rocks and lacustrine deposits unconformably overlie all the older rocks (Figs 1 and 2).

Characteristic blueschist facies mineral assemblages are best developed in the metabasites and metacherts of the blueschist sequence; these are described from several localities in north-west Turkey (e.g. Çoğulu, 1967; Okay, 1980a,b; Kulaksız, 1981; Monod *et al.*, 1991). The lower, metaclastic part of the blueschist sequence investigated here, containing jadeite-bearing schists, outcrops largely in the western extremity of the Tavşanlı Zone along the Kocasu river (Fig. 1).

FIELD RELATIONS

In the Kocasu region a steeply dipping fault east of the village of Alpagut, with post-Miocene strike-slip activity, represents the Neo-Tethyan oceanic suture. It separates unmetamorphosed Mesozoic rocks of the upper, northern plate (the Sakarya Zone) from the Cretaceous blueschists in the south (Figs 1 and 2). Rocks north-west of the suture consist of a thick, strongly deformed Triassic greywacke sequence with Permian limestone blocks (the Orhanlar Greywacke). They are unconformably overlain by Jurassic clastics and carbonates (Fig. 1). Peridotite, the volcanosedimentary sequence and blueschists, to be described below, constitute the rock units south-east of the suture.

Peridotite. The ultramafic rocks consist of massive, partly serpentinized spinel harzburgite, which are cut by 1–5-m-thick microgabbroic dykes, that do not extend down into the volcanosedimentary sequence. The dyke mineralogy consists of augite, partially to completely replaced by magmatic hornblende,

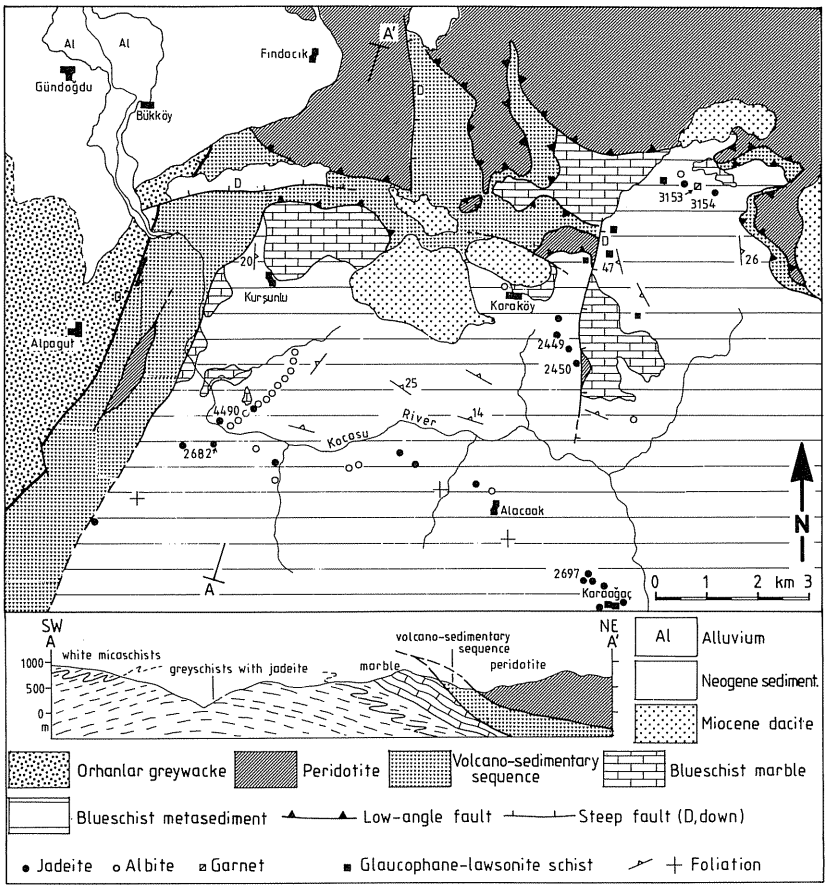

Fig. 2. Geological map and cross-section of the Kocasu region with specimen localities. Sample 4365B comes 300 m south of the village of Karaağaç.

and saussuritized plagioclase; the mineral assemblage in the dykes indicates that the dykes and, by inference, the ultramafic body, have not undergone blueschist facies metamorphism. The ultramafic body overlies the volcanosedimentary sequence along a shallowly dipping, sharp fault contact (Fig. 2).

Volcanosedimentary sequence. This comprises spilitized basic volcanic and pyroclastic rocks, with lesser amounts of radiolarian chert and pelagic shale, and very minor pelagic limestone and serpentinite that form imbricate tectonic slices. A slice of red, micritic, pelagic limestone intercalated with radiolarian cherts, a few kilometres north of the area in Fig. 2, contains the microfossil *Pithonella ovalis,* indicative of a Cenomanian to Maastrichtian age.

The volcanosedimentary sequence is cut by numerous shear zones with tens to hundreds of metres spacing. Apart from local development of foliation along these shear zones, the rocks in the volcanosedimentary sequence are free of penetrative deformation. With its tectonic and lithological features, the volcanosedimentary sequence represents a sediment-starved Cretaceous accretionary complex at the northern margin of the Tethys ocean made up of accreted slices of the upper layers of oceanic crust. Such volcanosedimentary sequences are common in north-west Turkey and are often called ophiolitic melange although they lack a well-defined matrix.

Mineral assemblages in the spilitized basic volcanic rocks in the volcanosedimentary sequence are characterized by titanian augite, albite and chlorite. The metamorphic minerals, apart from albite and chlorite, are pumpellyite and aragonite which commonly fill amygdules. No sodic pyroxene or lawsonite were recognized in the study area, although they are present in similar volcanosedimentary sequences north-east of Tavşanlı (Okay, 1982).

Blueschists. Blueschist assemblages characterize a largely metaclastic sequence over 1000 m thick, overlain by massive white marble, exposed along the deeply carved Kocasu river valley (Fig. 2). The rocks are completely recrystallized, medium grained and show a well-developed penetrative foliation and a distinct late crenulation cleavage. Early isoclinal folds are modified by open folds related to the crenulation cleavage. The sequence can be divided into two parts: an upper section, a few hundred metres thick, consists of white, strongly foliated, fine- to medium-grained metapelitic mica schists of white mica and quartz. Thin metabasite and marble horizons occur locally in the upper parts of the mica schists near the contact with the overlying marble (Fig. 2). The more massive lower section of the metaclastic sequence, over 800 m thick, termed greyschists, is made up of grey, graphite-bearing, quartz-rich, locally finely banded gneissic schists with jadeite, glaucophane, chloritoid and white mica. Mica schists and greyschists contain up to several-metres-thick, white to pale grey, massive or finely banded layers or boudins of jadeite and quartz with minor phengite. From their unusual composition and banded nature, these jadeite schist layers might have originally been ignimbrite flows. The whole blueschist sequence is cut by ubiquitous quartz veins a few centimetres wide and is intruded by Miocene dacite plugs (Fig. 2).

PETROGRAPHY

The greyschists represent metamorphosed sandstones and siltstones. However, their bulk composition, as inferred from mineral assemblages, is strikingly different from that of the average sandstone or shale (cf. Pettijohn, 1975) in

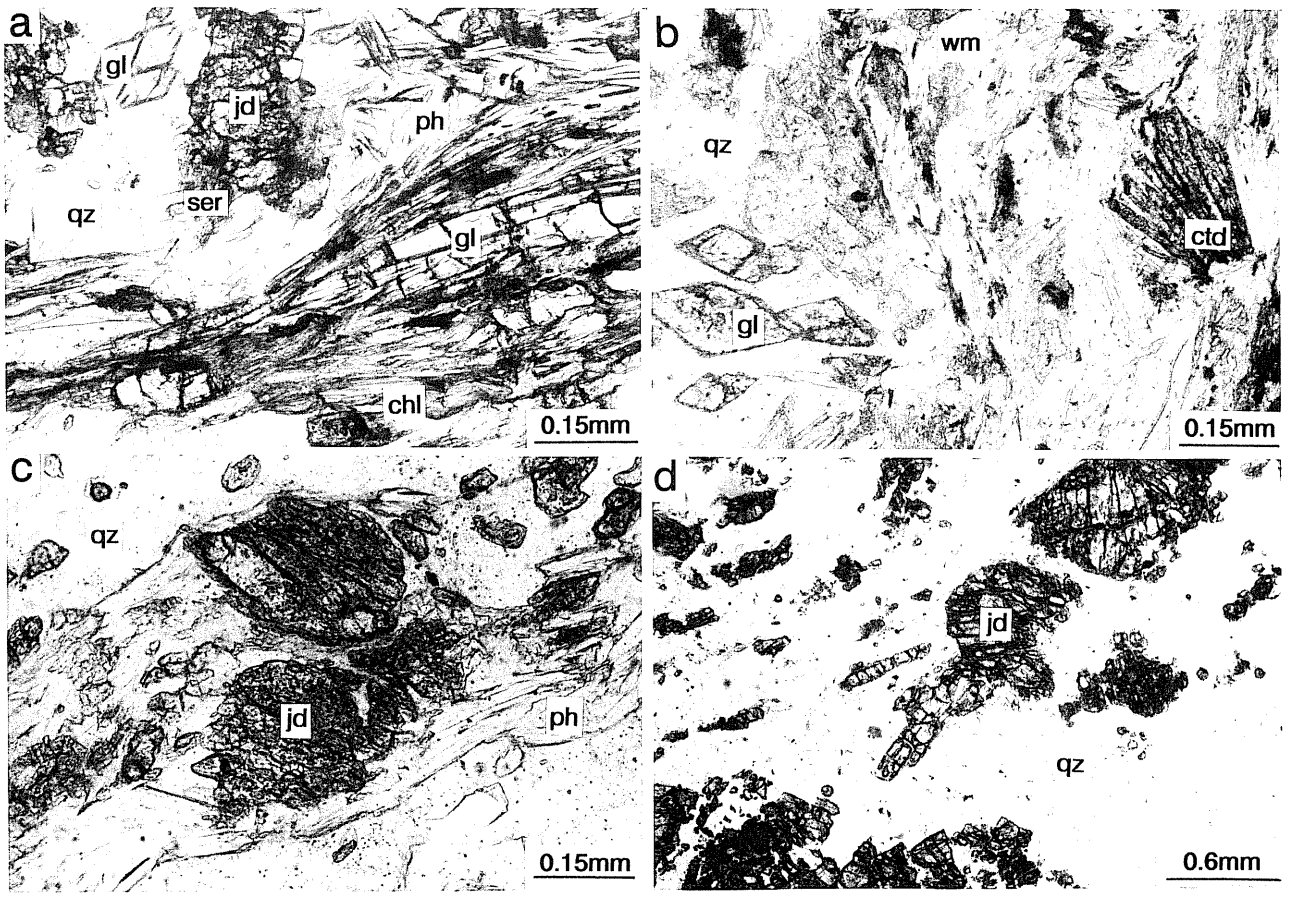

Fig. 3. Photomicrographs from the Kocasu blueschists (plane polarized light). (a) Glaucophane–jadeite schist (4490C) with glaucophane (gl), jadeite (jd) partially replaced by sericitic muscovite (ser), phengite (ph), chlorite (chl) and quartz (qz). (b) Glaucophane–chloritoid schist (4365B) with chloritoid (ctd), glaucophane (gl) with oxychlorite rims, white mica (wm) and quartz (qz). (c) Jadeite schist (2449) with 100 mol% jadeite (jd), phengite (ph) and quartz (qz). Phengites from this sample yielded an Ar/Ar age of 89 Ma. (d) Jadeite rock (2697A) with jadeite (jd) and quartz (qz). The dark colour of the jadeite grains is caused by very fine-grained, disseminated opaque minerals.

Table 1. Estimated modal abundances of the analysed specimens.

	Jadeite-rock			Jadeite–glaucophane schist			Chloritoid schist		Lawsonite–actinolite schist
	2697A	2449	2682	2450E	3154	4490C	2450B	4365B	3153
Quartz	46	35	38	29	25	41	34	22	—
White mica	1	20m	17m	15m,p	20m	25m	43m,p	35m,p	—
Jadeite	53	45	39	46	39	5	—	—	—
Lawsonite	—	—	—	—	—	—	—	—	39
Na-amphibole	—	—	—	6	7	9	ps	18	—
Actinolite	—	—	—	—	—	—	—	—	46
Garnet	—	—	—	—	—	—	—	—	4
Chlorite	—	—	—	3	8	14	14	5	5
Chloritoid	—	—	—	—	—	—	7	9	—
Graphite	—	—	—	tr	tr	tr	2	7	—
Opaque	—	—	1_a	$tr_{a,b}$	tr_b	tr_a	1_a	tr_a	—
Rutile	—	—	—	tr	tr	—	tr	—	—
Titanite	—	—	—	—	—	—	—	—	6
Apatite	—	—	—	tr	—	—	tr	—	—
Albite	—	—	5	tr	1	6	tr	3	—

m, phengite; p, paragonite; a, pyrite; b, ilmenite. tr < 0.1; ps, chlorite pseudomorphs after sodic amphibole.

being rich in sodium and almost free of both calcium and ferric iron.

The common mineral assemblage in the greyschists is quartz + phengite + jadeite ± glaucophane ± chlorite ± paragonite ± graphite (Fig. 3a). Quartz, white mica and jadeite are dominant in the mode (Table 1). Large quartz grains show recrystallization to finer crystal aggregates. White mica forms millimetre-thick bands composed of small (0.1–0.2 mm) grains, defining the foliation; electron microprobe analyses show that paragonite and phengite are interlayered on a micrometre scale in several samples (cf. Shau *et al.*, 1991). Jadeite forms irregular equant crystals up to 8 mm in size that are often turbid due to fine dense fractures and inclusions of very fine-grained opaque minerals. Sodic amphibole occurs as 0.5–2-mm-long, idioblastic, colourless to pale blue grains, aligned parallel to the foliation (Fig. 3a). Although most of the chlorite is clearly secondary, replacing sodic amphibole, chlorite also occurs in mica bands in apparent equilibrium with phengite and paragonite. However, no stable jadeite–chlorite contacts were observed.

A rare but petrogenetically important assemblage in the greyschists is quartz + phengite + paragonite + chloritoid + gluacophane ± chlorite + graphite. Chloritoid occurs as 1-mm-long, splaying, loose rosettes of pale bluish green, slender, prismatic crystals that are associated with white mica (Fig. 3b). Chloritoid and glaucophane are partly replaced by chlorite. However, chlorite also occurs in mica and graphite bands in apparent equilibrium with these minerals. Garnet, carpholite and talc are noticeably absent in over 110 thin sections of greyschists that were petrographically examined.

The mineral assemblage in jadeite schist is jadeite + quartz + phengite. The banded variety, exemplified by sample 2449, consists of prismatic jadeite up to 0.5 mm in size, quartz and phengite bands (Fig. 3c) alternating with quartz bands. The massive jadeite schists consist of prismatic or splaying aggregates of jadeite up to 5 mm in size with quartz and very minor phengite (Fig. 3d). Jadeite constitutes over 85% of some rocks.

The mineral assemblage in the metabasic rocks in the upper part of the blueschist sequence is sodic amphibole + lawsonite + chlorite + titanite ± sodic pyroxene ± phengite ± quartz. Texturally and mineralogically they are very similar to the metabasites described from north-east of Tavşanlı (Okay, 1980a).

A massive, fine-grained layer several metres thick with the mineral assemblage actinolite + lawsonite + garnet + chlorite + titanite occurs within the grey schists in the northern part of the study area (Fig. 2). The actinolite–lawsonite schist (sample 3153), which may represent a metamorphosed marl, consists of interlocking colourless actinolite 0.2 mm in size, pale green chlorite and prismatic lawsonite. Almandine–grossular garnet with a significant spessartine component constitutes only 4% of the rock and forms idioblastic grains 0.1 mm in size. Apart from this rock, garnet is notably absent in the study area.

The alteration of greyschists and jadeite schists is sporadic and does not show a clear geographical pattern. Jadeite is frequently replaced by very fine-grained aggregates of sericitic muscovite (Fig. 3a) rather than albite, which forms clear crystals with lamellar or checkerboard twinning in the quartz groundmass. Sodic amphibole is commonly altered to brownish oxychlorite (Fig. 3b). The alteration is not associated with penetrative deformation, and the former presence of jadeite and sodic amphibole can easily be recognized by their pseudomorphs.

METHODS

Mineral compositions in nine samples from the Kocasu region were analysed with an SX-50 Cameca electron microprobe in the Department of Earth Sciences at Cambridge University, UK. The estimated modes of the analysed samples are given in Table 1. Operating conditions were 20-kV accelerating voltage, 10-nA beam current and 10-μm beam size. The elements were analysed with energy- and wavelength-dispersive spectrometers. Mineral reactions were calculated using THERMOCALC (Holland & Powell, 1990) with end-member activities based on ideal mixing on sites, unless stated otherwise.

Two jadeite schist samples with the mineral assemblage jadeite + quartz + phengite (samples 2449 and 2682, cf. Figs 2 and 3c) were dated by an argon laser probe at the Open University, UK. The simple mineral assemblage of the specimens ensures little celadonitic re-equilibration. Phengites from both specimens are of similar grain size (about 0.1 mm) and only those from sample 2449 show some recrystallization to finer grained aggregates. They are associated with 0.3-mm jadeite and quartz. Phengites from both specimens have relatively constant Si contents (cf. Fig. 7), suggesting little alteration.

Rock slices of both samples (10 × 10 × 1-mm) were polished on one side and cleaned ultrasonically in methanol before being wrapped in aluminium foil for irradiation. The samples received 10^{18} neutrons cm^{-2} at the Ford Reactor, Michigan, monitored using the MMhb1 hornblende standard (520.4 Ma, Samson & Alexander, 1987). The calculated J value for the sample was 0.0104 ± 0.00005.

The sample was loaded into the ultrahigh-vacuum laser port and heated to reduce atmospheric blank levels. Argon was extracted from small areas using short pulses (10–100 ms), produced by a computer-controller external shutter and a Spectron SL902 CW Nd-YAG laser producing up to 17 W TEM_{00}. The beam was directed into a customized Leica Metallux 3 microscope and focused at the sample surface via the objective lens. The sample was observed using a CCD camera coaxial with the laser beam. Gases released by the laser were gathered for 5 min, and then allowed into a MAP 215-50 noble gas mass spectrometer. Peaks between 35 and 41 were scanned seven times and amounts extrapolated back to the inlet time. Blanks were analysed after every sample extraction. The resulting analyses were corrected for blanks, ^{37}Ar decay and neutron-induced interferences. The correction factors used were: $(^{39}Ar/^{37}Ar)Ca = 0.000781 \pm 0.000053$; $(^{36}Ar/^{37}Ar)Ca = 0.000205 \pm 0.000022$; $(^{40}Ar/^{39}Ar)K = 0.031 \pm 0.008$, based upon analyses of calcium and potassium salts.

MINERAL CHEMISTRY

Jadeite. Structural formulae for jadeite were calculated on the basis of four cations; the jadeite component is taken to be equal to Al^{VI}; the aegirine component equals $Na/(Na + Ca) - Al^{VI}$. The rest is assigned to the augite component. On this basis jadeite in all the analysed samples contains over 85 mol% jadeite component (Table 2, Fig. 4); the rest is largely aegirine (1–7%)

Table 2. Representative mineral compositions from the Kocasu region.

	Jadeite						Sodic amphibole				Actinolite	Chloritoid		Garnet	
	2449	2450E	2682	2697	3154	4490C	2450E	3154	4365B	4490C	3153	2450B	4365B	3153	
SiO_2	58.45	58.88	59.66	58.93	58.74	58.43	58.26	56.07	58.19	58.29	55.35	22.66	24.13	37.36*	37.25†
TiO_2	0.00	0.25	0.06	0.08	0.50	0.15	0.03	0.01	0.09	0.00	0.03	0.02	0.00	0.00	0.16
Al_2O_3	25.72	22.98	24.72	25.12	24.05	23.04	12.10	11.08	11.61	12.15	0.38	39.00	40.36	20.89	20.85
Cr_2O_3	0.02	0.02	0.00	0.01	0.03	0.00	0.00	0.05	0.00	0.01	0.01	0.03	0.06	0.00	0.10
FeO	0.05	2.02	0.82	0.83	2.24	2.46	7.92	15.63	11.38	8.82	10.12	24.75	24.17	21.28	21.77
MgO	0.01	0.79	0.00	0.05	0.13	0.26	10.37	6.31	8.69	10.07	17.37	1.92	2.49	1.11	0.64
MnO	0.01	0.02	0.00	0.00	0.00	0.02	0.01	0.01	0.02	0.09	0.19	0.39	0.72	9.86	5.80
CaO	0.04	1.04	0.03	0.12	0.18	0.48	0.00	0.08	0.02	0.01	13.31	0.05	0.00	9.18	13.64
Na_2O	15.16	14.17	15.15	15.06	14.88	14.43	7.36	7.02	7.44	7.06	0.14	0.01	0.10	0.28	0.05
K_2O	0.02	0.01	0.00	0.00	0.03	0.02	0.04	0.04	0.00	0.03	0.01	0.01	0.00	0.00	0.00
Total	99.48	100.18	100.44	100.20	100.78	99.29	96.09	96.30	97.44	96.53	96.91	88.84	92.03	99.96	100.26
Structural formula based on:															
	4 cat	4 cat		4 cat	4 cat		23 ox	23 ox	23 ox	23 ox	23 ox	12 ox	12 ox	12 ox	12 ox
Si	1.98	2.00	2.01	1.99	1.98	2.01	8.02	7.98	8.02	8.01	7.94	1.97	2.01	3.00	2.97
Al^{IV}	0.02	0.00	0.00	0.01	0.02	0.00	0.00	0.02	0.00	0.00	0.06	0.03	3.00	0.00	0.03
Al^{VI}	1.00	0.92	0.98	0.99	0.94	0.93	1.96	1.84	1.88	1.97	0.00	3.95	0.96	1.98	1.93
Ti	0.00	0.01	0.00	0.00	0.01	0.00	0.00	0.00	0.01	0.00	0.00	0.00	0.00	0.00	0.01
Cr	0.00	0.00	0.00	0.00	0.00	0.00	0.00	0.00	0.00	0.00	0.00	0.00	0.00	0.00	0.01
Fe^{3+}	0.00	0.04	0.02	0.01	0.06	0.07	0.00	0.10	0.02	0.00		0.04	0.04	0.02	0.05
Fe^{2+}	0.00	0.02	0.00	0.01	0.01	0.00	0.91	1.76	1.30	1.02	1.22	1.75	1.64	1.40	1.40
Mg	0.00	0.04	0.00	0.00	0.01	0.01	2.13	1.34	1.78	2.07	3.72	0.25	0.31	0.13	0.08
Mn	0.00	0.00	0.00	0.00	0.00	0.00	0.00	0.00	0.00	0.01	0.02	0.03	0.05	0.67	0.39
Ca	0.00	0.04	0.00	0.00	0.00	0.00	0.00	0.01	0.00	0.00	2.05	0.01	0.00	0.79	1.17
Na	1.00	0.94	0.99	0.98	0.97	0.96	1.96	1.94	1.99	1.88	0.04	0.00	0.02	0.04	0.00
K	0.00	0.00	0.00	0.00	0.00	0.00	0.01	0.01	0.00	0.00	0.00	0.00	0.00	0.00	0.00
Total	4.00	4.00	4.00	3.99	4.00	3.98	14.99	15.00	15.00	14.96	15.05	8.03	8.03	8.03	8.04
													alm	46.8	46.1
jd	100.0	92.1	97.9	98.5	93.7	93.2							pyr	4.4	2.5
aeg	0.0	4.0	2.0	1.1	5.7	6.7							spess	22.4	12.9
au	0.0	3.9	0.1	0.4	0.6	0.1							gros	26.4	38.5

* Core, † rim.

with a very minor augite component. Jadeite from sample 2449 is 100 mol% jadeite.

Sodic amphibole. Structural formulae for sodic amphibole were calculated on the basis of 15 cations and 23 oxygens. Sodic amphiboles from greyschists are glaucophane–ferroglaucophane solid solutions, with very minor ferric iron and calcium as shown by the Ca/(Ca + Na) ratios <0.01 (Fig. 5, Table 2). Only sodic amphiboles from the chloritoid schist show a slight zoning involving an increase in Al^{VI} towards the rim (Fig. 5).

Chloritoid. Representative chloritoid compositions are given in Table 2. Fe^{3+} was estimated assuming four trivalent atoms. Chloritoid is Fe^{2+}-rich, with $Fe^{2+}/(Fe^{2+} + Mg)$ ratios of over 0.84. It shows no zoning and contains minor Mn and Fe^{3+}.

Chlorite. Chlorite compositions are shown in Fig. 6 and representative chlorite analyses are given in Table 3. Chlorite from the greyschists shows a range of Fe/(Fe + Mg) ratios (0.45–0.75) and is richer in Fe and Al compared with chlorite from the metabasites of the same metamorphic grade (cf. Okay, 1980a).

Phengite. Phengite compositions from the metasediments are shown in terms of Si and (Fe + Mg + Mn) per formula unit (pfu) in Fig. 7, and representative compositions are given in Table 3. The maximum Si content is 3.56 pfu. The lower Si values recorded in jadeite schists are due to the Fe- and Mg-poor nature of their protoliths. The deviation of phengite composition from the ideal celadonite–muscovite join in jadeite–glaucophane schists suggests the presence of Fe^{3+} in phengites from these rock types (Fig. 7).

Paragonite. Uncontaminated paragonite analyses are difficult to obtain due to the finely interlayered nature of phengite and paragonite. Purest paragonite analyses record about 10 mol% phengite substitution (Table 3).

Garnet. Garnet from the lawsonite–actinolite schist sample 3153, although only 0.1 mm across, shows a marked prograde zoning involving an increase in grossular content at the expense of spessartine and pyrope towards the rim (Table 2).

Actinolite. Actinolite from sample 3153 is close to the ideal structural formula with very minor Al and Na (Table 2).

Lawsonite. Lawsonite compositions are close to the ideal structural formula with only minor substitution of Al by Fe^{3+} (Table 3).

The relative Fe/Mg values in the metasedimentary rocks are chloritoid ≫ chlorite > sodic amphibole > phengite.

PHASE RELATIONS

As phengite is the only potassic phase in the greyschists, the remaining major phases, jadeite, sodic amphibole,

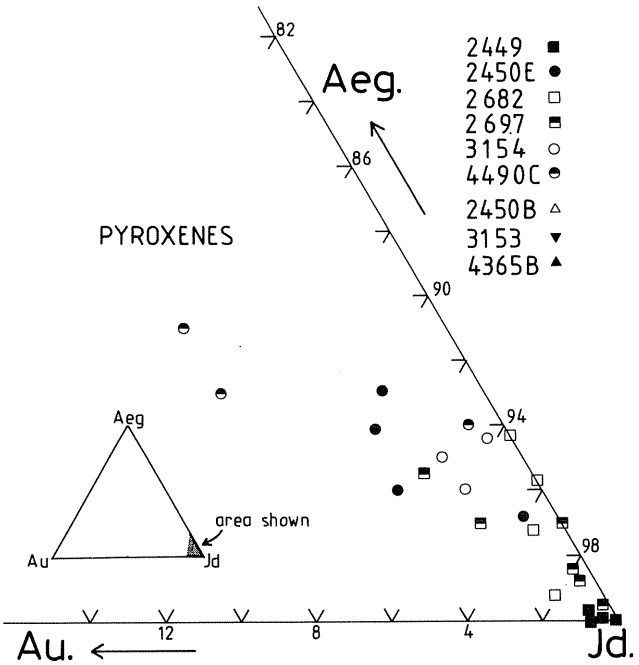

Fig. 4. Jadeite compositions from the Kocasu region plotted in the jadeite corner of the aegirine ($NaFeSi_2O_6$)–jadeite($NaAlSi_2O_6$)–augite[$Ca(MgFeMn)Si_2O_6$] ternary diagram.

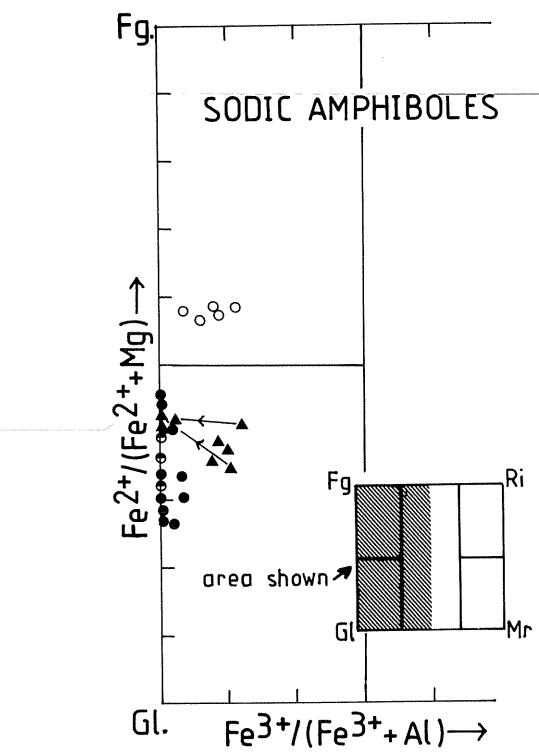

Fig. 5. Sodic amphibole compositions from the Kocasu region plotted on part of the Miyashiro diagram. Arrows indicate core to rim compositions. Fg, ferroglaucophane; Gl, glaucophane; Mr, magnesioriebeckite; Ri, riebeckite. Other symbols as in Fig. 4.

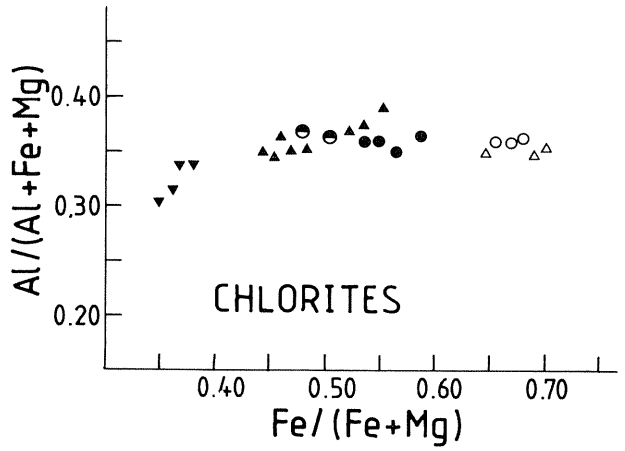

Fig. 6. Chlorite compositions from the Kocasu region shown in terms of Al/(Al + Fe + Mg) versus Fe/(Fe + Mg). Symbols as in Fig. 4.

paragonite, chloritoid, chlorite and quartz, can be described in the Na_2O–FeO–MgO–Al_2O_3–SiO_2–H_2O system (NFMASH). A Schreinemakers diagram can be used to analyse the relation between these six minerals and a fluid phase using the ferrous and magnesian end-members of sodic amphibole, chloritoid and chlorite. A Schreinemakers bundle for the NFASH system for seven phases and five components, constructed using THERMOCALC (Holland & Powell 1990), is shown in Fig. 8. The Schreinemakers diagram defines five P–T fields for quartz-bearing parageneses. The phase relations in these fields are shown in Na–Al–Fe ternary diagrams (NAF) as projected from quartz and H_2O. Reactions for the magnesian end-members fall largely outside the stability field of paragonite and in the stability field of coesite, introducing added complexities.

The observed critical high-variant mineral assemblages in the Kocasu region, jadeite + glaucophane + paragonite + quartz and glaucophane + chloritoid, and the absence of the jadeite + chloritoid assemblage, indicates that the phase relations in this region correspond to the segment between reactions (1) and (2) on the Schreinemakers diagram (Fig. 8).

The lower pressure stability limit of the chloritoid + glaucophane assemblage is given by the reaction

$$\text{chloritoid} + \text{glaucophane} + H_2O = \text{paragonite} + \text{chlorite} + \text{quartz}. \quad (1)$$

This reaction was calculated by El-Shazly & Liou (1991) using GE0-CALC software (Berman, 1988) with modified thermodynamic data, and by Guiraud *et al.* (1990) using THERMOCALC. El-Shazly & Liou (1991) place the reaction well into the albite stability field in the NFASH system, while Guiraud *et al.* (1990) conclude that the chloritoid + glaucophane assemblage is only stable in the jadeite stability field. In the Kocasu region, Fe^{2+}-rich chloritoid ($X_{Fe} \geq 0.85$) coexists with glaucophane in the

Table 3. Representative mineral analyses from the Kocasu region.

	Chlorite						Phengite					Paragonite		Lawsonite
	2450B	2450E	3153	3154	4365B	4490C	2449	2450E	2682	3154	4365B	2450E	4365B	3153
SiO_2	24.71	25.28	27.26	24.43	26.63	27.16	48.96	50.11	51.44	51.91	52.93	46.76	47.25	37.52
TiO_2	0.00	0.03	0.02	0.03	0.01	0.00	0.25	0.05	0.10	0.06	0.10	0.00	0.03	0.05
Al_2O_3	19.34	20.41	17.92	20.02	20.09	20.30	28.66	25.28	25.65	23.09	24.05	38.51	37.48	32.56
Cr_2O_3	0.00	0.00	0.11	0.01	0.01	0.00	0.00	0.05	0.02	0.01	0.09	0.04	0.00	0.04
FeO	34.13	28.19	20.09	32.81	24.44	23.63	2.75	2.16	3.64	3.95	2.45	0.76	0.60	0.64
MgO	8.60	13.04	19.96	9.73	16.43	14.60	2.04	3.71	2.77	3.86	4.34	0.48	0.40	0.04
MnO	0.27	0.05	0.25	0.14	0.12	0.39	0.27	0.04	0.03	0.00	0.00	0.01	0.00	0.02
CaO	0.03	0.02	0.06	0.00	0.00	0.20	0.02	0.03	0.00	0.00	0.00	0.09	0.03	17.71
Na_2O	0.13	0.01	0.01	0.02	0.03	0.01	0.19	0.20	0.00	0.00	0.00	6.41	5.70	0.00
K_2O	0.00	0.03	0.02	0.01	0.00	0.04	10.95	10.64	11.39	10.89	10.58	1.13	1.01	0.00
Total	87.21	87.06	85.70	87.20	87.76	86.33	94.09	92.27	95.04	93.77	94.54	94.19	92.50	88.58
Structural formula based on:														
	14 ox	14 ox	14 ox	14 ox	14 ox	14 ox	11 ox	11 ox	11 0x	11 ox	11 ox	11 ox	11 ox	8 ox
Si	2.76	2.73	2.87	2.71	2.79	2.87	3.33	3.46	3.47	3.55	3.55	3.03	3.09	1.97
Al^{IV}	1.24	1.27	1.13	1.29	1.21	1.13	0.67	0.54	0.53	0.45	0.45	0.97	0.91	0.03
Al^{VI}	1.31	1.32	1.09	1.32	1.26	1.40	1.63	1.51	1.52	1.42	1.46	1.97	1.98	1.99
Ti	0.00	0.00	0.00	0.00	0.00	0.00	0.01	0.00	0.01	0.00	0.01	0.00	0.00	0.00
Cr	0.00	0.00	0.01	0.00	0.00	0.00	0.00	0.00	0.00	0.00	0.00	0.00	0.00	0.00
Fe	3.19	2.54	1.77	3.04	2.14	2.09	0.16	0.13	0.21	0.23	0.14	0.04	0.03	0.03
Mg	1.43	2.10	3.13	1.61	2.56	2.30	0.21	0.38	0.28	0.39	0.44	0.05	0.04	0.00
Mn	0.03	0.01	0.02	0.01	0.01	0.04	0.02	0.00	0.00	0.00	0.00	0.00	0.00	0.00
Ca	0.01	0.00	0.01	0.00	0.00	0.02	0.00	0.00	0.00	0.00	0.00	0.01	0.00	1.00
Na	0.03	0.00	0.00	0.01	0.01	0.00	0.03	0.03	0.00	0.00	0.00	0.80	0.72	0.00
K	0.00	0.01	0.00	0.00	0.00	0.01	0.95	0.94	0.98	0.95	0.91	0.09	0.08	0.00
Total	10.00	9.98	10.03	9.99	9.98	9.86	7.01	6.99	7.00	6.99	6.96	6.96	6.85	5.02

jadeite stability field, indicating that reaction (1) for Fe end-members should lie at higher pressures than that shown by El-Shazly & Liou (1991).

Reactions (1)–(3) in Fig. 8 are limited at high temperature (480–500 °C) by the formation of garnet through the reaction

$$\text{chloritoid} + \text{chlorite} + \text{quartz} = \text{garnet} + H_2O \quad (6)$$

Guiraud *et al.* (1990) place reaction (6) at lower temperatures than the invariant point f1 in Fig. 8, thereby rendering the invariant point and reactions (1)–(3) metastable. In contrast to this, the coexistence of chloritoid + glaucophane + chlorite + quartz without garnet in the Kocasu region indicates that reaction (6) occurs at higher temperatures than the invariant point f1, even in rocks free of Fe_2O_3 (cf. fig. 4 of Guiraud *et al.*, 1990). Nevertheless, the chloritoid + glaucophane paragenesis without garnet in the NFMASH system has a very narrow thermal stability field and is limited at high temperatures by the garnet-forming reactions (7) and (8) (Fig. 8):

$$\text{chloritoid} + \text{glaucophane} = \text{jadeite} + \text{garnet} + \text{quartz} + H_2O, \quad (7)$$

$$\text{chloritoid} + \text{glaucophane} + \text{quartz} = \text{garnet} + \text{paragonite} + H_2O. \quad (8)$$

This explains the rarity of chloritoid + glaucophane parageneses in the absence of garnet. Apart from the Kocasu region, the Peloponnese apparently is the only place where this paragenesis is recorded (Theye & Seidel, 1991), although chloritoid + glaucophane + garnet assemblages are relatively widespread in some blueschist

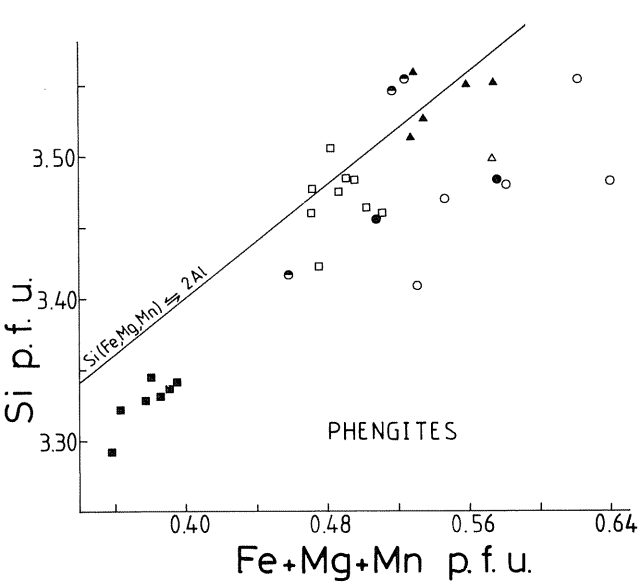

Fig. 7. Phengite compositions from the Kocasu region shown in terms of Si and (Fe + Mg + Mn) per formula unit (pfu). The ideal celadonite–muscovite substitution line is also shown. Symbols as in Fig. 4.

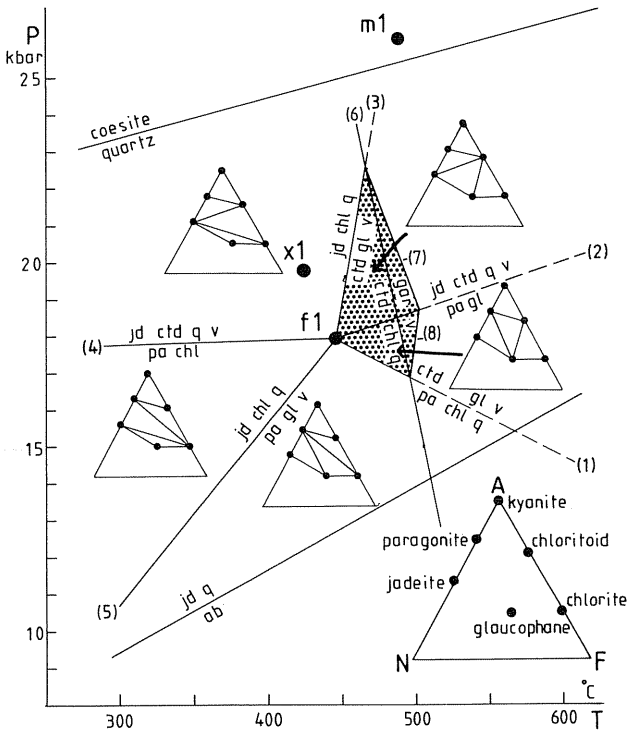

Fig. 8. Schreinemakers diagram for the NFASH system for the end-members jadeite (jd), ferroglaucophane (gl), paragonite (pa), ferrochloritoid (ctd), daphnite (chl), quartz (q) and H_2O (v). Some other relevant equilibria and three garnet-forming reactions (6–8) are also marked. Two reactions that are not labelled are ctd + gl = jd + gar + q + v (7), and ctd + gl + q = gar + pa + v (8); f1, m1 and x1 indicate the invariant points in the NFASH system, NMASH system and for real mineral compositions from specimen 4365B, respectively. The stability field of chloritoid + glaucophane without garnet is stippled. Other abbreviations: ab, albite; gar, garnet. Reactions (1)–(3) are metastable to the right of the garnet-forming reaction and are shown as broken lines. All reactions were calculated using THERMOCALC of Holland & Powell (1990).

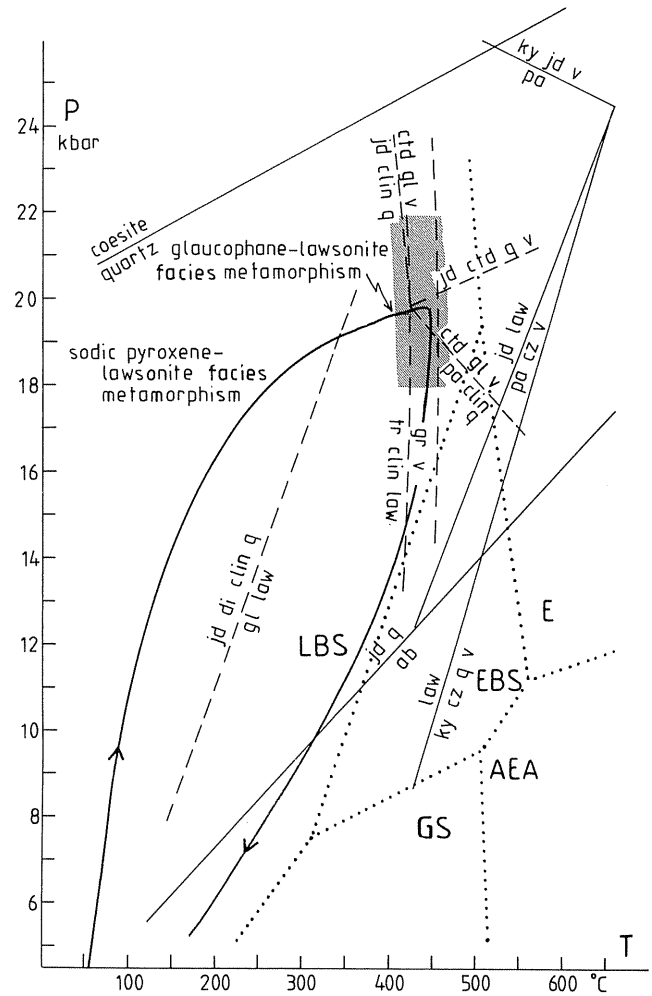

Fig. 9. Pressure–temperature diagram showing equilibria relevant to the estimation of the *P–T* conditions of the Kocasu greyschists and their probable *P–T* path. Facies boundaries are after Evans (1990); LBS, lawsonite blueschist; EPS, epidote blueschist; E, eclogite; AEA, albite–epidote amphibolite; GS, greenschist facies. Dashed lines around the invariant point indicate reactions calculated using Mg end-members of real mineral compositions from samples 4365B and 3153, while solid lines are end-member reactions. The two reactions involving garnet are for different pyrope activities. Reaction (13) is calculated using mineral compositions from the lawsonite-zone metabasites from north-east of Tavşanlı (activities used, jd 0.37, di 0.13, gl 0.10, clin 0.126). All reactions were calculated using THERMOCALC of Holland & Powell (1990). Abbreviations: ab, albite; clin, clinochlor; ctd, chloritoid; cz, clinozoisite; di, diopside; gl, glaucophane; ky, kyanite; jd, jadeite; law, lawsonite; pa, paragonite; q, quartz; tr, tremolite; v, H_2O.

terranes (cf. El-Shazly & Liou, 1991). Part of the reason for this is because garnet will form at lower temperatures in rocks with Ca and Mn and thus will overprint the *P–T* field of chloritoid + glaucophane without garnet in most rock compositions.

P–T CONDITIONS AND *P–T* PATH

The jadeite + paragonite + quartz assemblage in the Kocasu region constrains the pressure between 12 and 25 kbar by three reactions (Fig. 9):

$$\text{albite} = \text{jadeite} + \text{quartz}, \quad (9)$$

$$\text{paragonite} = \text{jadeite} + \text{kyanite} + H_2O, \quad (10)$$

$$\text{quartz} = \text{coesite}. \quad (11)$$

Phengites with up to 3.56 Si pfu in the greyschists indicate minimum pressures of 14 kbar according to the phengite geobarometer of Massonne & Schreyer (1987). Equilibrium (1) is pressure sensitive and provides a useful geobarometer (cf. Theye & Seidel, 1991). All the minerals in this equilibrium are present in specimen 4365B (Table 2). Using ideal activity models for Mg end-members in the THERMOCALC program, pressure is constrained to be 20 ± 2 kbar at 430° C (Fig. 9). Reaction for the Fe end-members yields about 2 kbar higher pressures. The nature of chlorite is ambiguous as a primary mineral in the jadeite-bearing schists, and if chlorite were not part of the

primary mineral assemblage, the above pressure would be a minimum value.

The stability of lawsonite and jadeite, a paragenesis observed in some greyschists in the Kocasu region, gives a maximum temperature of 560° C at 20 kbar (Fig. 9). Minimum temperatures of 420° C at 20 kbar are given by the stable coexistence of chloritoid and glaucophane in specimen 4365B through the equilibrium (Fig. 9)

$$\text{chloritoid} + \text{glaucophane} + H_2O = \text{jadeite} + \text{quartz} + \text{chlorite}. \quad (3)$$

An independent estimate of temperature is given by the mineral equilibrium in the actinolite–lawsonite schist:

$$\text{tremolite} + \text{chlorite} + \text{lawsonite} = \text{garnet} + H_2O. \quad (12)$$

Reaction (12) was calculated for mineral compositions from specimen 3153 (cf. Table 2) using ideal activities based on mixing-on-sites. This reaction has a subvertical slope in the P–T field and for Mg end-members indicates a temperature of 415°C for a wide pressure range of 13–25 kbar (Fig. 9). If pyrope activities based on the Newton & Haselton (1981) activity model are used, which entails a fourfold increase in the activity of pyrope, the temperature of reaction (12) increases to 445° C (Fig. 9).

The transition from lawsonite blueschist facies to epidote blueschist and eclogite facies occurs between 450 and 500° C (Evans, 1990). The P–T conditions for eclogite blueschist and epidote blueschist facies rocks from the Cyclades with garnet, omphacite and epidote parageneses in metabasites were 470 ± 30° C and 15 ± 3 kbar (e.g. Schliestedt, 1986; Okrusch & Bröcker, 1990). The temperatures in the Kocasu region, where the metabasic mineral paragenesis is sodic amphibole + lawsonite generally without epidote, must therefore have been <450° C. Epidote is a rare and probably secondary mineral in the Kocasu region, and it is generally found in altered greyschists associated with albite and chlorite.

Taking these factors into account, we therefore estimate that P–T conditions of blueschist metamorphism in the Kocasu area were 430 ± 30° C and 20 ± 2 kbar (Fig. 9).

Metabasic rocks from north-east of Tavşanlı show two stages of metamorphism. An initial static stage is characterized by sodic pyroxene + lawsonite + chlorite + quartz, where sodic pyroxene often pseudomorphs the igneous augite. In the second stage associated with penetrative deformation, sodic amphibole forms at the expense of sodic pyroxene, chlorite and quartz (Okay, 1980b). In the Kocasu region, the blueschist metabasites contain relict sodic pyroxene, indicating that they have followed a similar metamorphic path. The reaction to produce sodic amphibole is

$$\text{jadeite} + \text{diopside} + \text{clinochlore} + \text{quartz} = \text{glaucophane} + \text{lawsonite}. \quad (13)$$

This reaction was calculated using mineral compositions from north-east of Tavşanlı (cf. Okay, 1980b) and is shown in Fig. 9.

The general absence of garnet in metabasic and metapelitic rocks, the lack of common greenschist facies overprint textures, such as actinolite rims around sodic amphibole or replacement of lawsonite by epidote, and reaction (13) put tight constraints on the P–T path followed by the Tavşanlı Zone blueschists, and show that it remained largely in the blueschist facies field (Fig. 9).

GEOCHRONOLOGY

The jadeite schist sample 2449 yielded three laser spot ages from different phengite grains, within error of each other, at 88.5 ± 0.5 Ma. Sample 2682 yielded one age of 83.5 ± 1.6 Ma and two younger ages of 70.0 ± 1.2 and 71·5 ± 0.7 Ma (Table 4). The variability of ages from sample 2682 indicates the possibility of partial resetting of phengites in this sample.

Estimates for the blocking temperature of muscovite range from 350°C to about 420°C depending on the grain size and cooling rate (Robbins, 1972; van Blanckenburg *et al.*, 1989). Using a mean grain size of 0.1 mm for phengite and a range of very approximate cooling rates (10–100° C Ma^{-1}), blocking temperatures of 369° C (for 10° C Ma^{-1}) and 416° C (for 100° C Ma^{-1}) can be calculated for the Kocasu blueschists (Robbins, 1972). These blocking temperatures are close to the peak metamorphic temperature, so that the blueschist ages can be regarded as dating the high-P metamorphism.

The isotopic age of the high-P/low-T metamorphism is

Table 4. Phengite $^{40}Ar/^{39}Ar$ isotopic data from two jadeite schists from the Kocasu region.

Sample	Run	^{40}Ar	^{39}Ar	^{36}Ar	$\%^{40}Ar^*$	$^{40}Ar^*/^{39}Ar$	Age (Ma)
2449	v85	841.08	166.75	0.093	96.74	4.88 ± 0.03	89.3 ± 0.7
2449	v87	41.59	8.39	0.015	89.49	4.44 ± 0.57	81.4 ± 10.2
2449	v89	612.72	125.39	0.045	97.85	4.78 ± 0.03	87.6 ± 0.7
						Weighted mean	88.4 ± 0.51
2682	v79	286.01	57.25	0.085	91.22	4.56 ± 0.09	83.5 ± 1.6
2682	v81	361.83	86.24	0.103	91.60	3.84 ± 0.07	70.7 ± 1.2
2682	v83	876.74	100.38	0.331	88.85	3.89 ± 0.03	71.5 ± 0.7

J value = 0.0104 + 0.00005. * Amounts of ^{40}Ar, ^{39}Ar and $^{36}Ar \times 10^{-12}$ ccSTP.

compatible with the palaeontological data from the volcanosedimentary sequence considering that accretion of the oceanic crust at the subduction zone, now represented by the volcanosedimentary sequence, must have preceded the subduction and blueschist facies metamorphism of the continental crust. The blueschist metamorphism in the Tavşanlı zone is 50 Ma older than the Middle Eocene high-*P* metamorphism in the Cyclades (e.g. Maluski *et al.*, 1987; Wijbrans *et al.*, 1990), indicating, contrary to some views (e.g. Ridley, 1984), that there is no direct genetic connection between the two high-*P* complexes. It is also older than the mid-Eocene medium-*P* metamorphism in the Menderes Massif to the south (Satır & Friedrichsen, 1986).

CONCLUSIONS

The blueschist belt in north-west Turkey, with its thick metapelitic and marble units, represents a deeply subducted passive continental margin of the Tethys ocean. The depositional age of the protoliths to the blueschists is Palaeozoic to Mesozoic, while the age of the high-*P*/low-*T* metamorphism is Late Cretaceous. In this respect, the Tavşanlı Zone is distinctly different from the circum-Pacific blueschist terranes that consist of accreted oceanic crust and trench turbidites.

The lower metaclastic part of the blueschist sequence in the Kocasu region contains regional jadeite, chloritoid and glaucophane and allows a relatively precise determination of the blueschist facies conditions (20 ± 2 kbar, $430 \pm 30°$ C). These *P–T* conditions give overall geothermal gradients close to $5°\,C\,km^{-1}$, which is one of the lowest gradients yet recorded. Calculations of the thermal structure of a subduction zone suggest that such low geothermal gradients occur where shear stress, convergence rate and basal heat flux are low, and subduction angle and thermal conductivity are high (Peacock, 1992). In the initial stage of blueschist metamorphism in the Tavşanlı Zone, penetrative deformation was absent and the igneous textures were retained (Okay, 1980b), suggesting that the shear stress in the subducting slab was low. Furthermore, the rate of subduction of continental crust because of its greater buoyancy must have been slower than that of oceanic crust. Thus, these two features were probably responsible for the unusually low geothermal gradients created in the subducting continental slab.

The blueschists in north-west Turkey, metamorphosed at a depth of 70 km, are tectonically overlain by a volcanosedimentary sequence and spinel peridotite slices that have not been buried deeper than about 30 km, suggesting removal of 40 km of overburden between the blueschists and their tectonic cover. Similar tectonic relations involving blueschists tectonically overlain by unmetamorphosed or low-grade sequences, have been reported from many parts of the world (e.g. Platt, 1986; Jayko *et al.*, 1987), where such tectonic contacts are interpreted as normal faults, which might also be the case in the Tavşanlı Zone. In the Kocasu region the tectonic contacts between the blueschists and the volcanosedimentary complex are sharp, low-angle faults often characterized by narrow silicified zones, which prevents unambiguous determination of the shear sense along these faults. The blueschists and the overlying peridotite are intruded by granodiorites dated at 48–53 Ma (Ataman, 1972; Harris *et al.*, 1994), which provides an upper age limit for fault movement at the blueschist–peridotite interface. The mineral assemblages of the granodiorites and their contact aureole indicate that the granodiorites were emplaced at a depth of 10 km (Harris *et al.*, 1994), so that exhumation of the blueschists by normal faulting from a depth of 70 km to 10 km occurred during the Late Cretaceous and Palaeocene between 88 and 53 Ma. The blueschists were probably partly exposed in the Early to Middle Eocene, as neritic limestones of that age are transgressive over the peridotites north of Tavşanlı (Baş, 1986).

The preservation of the blueschist assemblages formed under unusually low geothermal gradients in the Kocasu region was possible probably by underplating of cold continental crustal material under the presently exposed blueschists while exhumation was proceeding by normal faulting at the blueschist–peridotite interface (e.g. Wijbrans *et al.*, 1993). The example of the Kocasu blueschists shows that geothermal gradients as low as $5°\,C\,km^{-1}$ can be created and preserved in subducted continental crust under favourable conditions.

ACKNOWLEDGEMENTS

Financial support for this study was provided by NATO Collaborative Research Grant 900412, TPAO and by TÜBİTAK Glotek grant. We thank A. El-din El-Shazly, J. Goodge and N. Harris for critically reviewing the manuscript. The Department of Earth Sciences in Cambridge is thanked for the use of the microprobe analyser facility.

REFERENCES

Ataman, G., 1972. Radiometric age of the granodiorite massif of Orhaneli (in Turkish). *Türkiye Jeoloji Kurumu Bülteni*, **15**, 125–130.

Baş, H., 1986. Tertiary geology of the Domaniç-Tavşanlı-Kütahya-Gediz region (in Turkish). *Jeoloji Mühendisliği*, **27**, 11–18.

Berman, R. G., 1988, Internally-consistent thermodynamic data for minerals in the system Na_2O–K_2O–CaO–MgO–FeO–Fe_2O_3–Al_2O_3–SiO_2–TiO_2–H_2O–CO_2. *Journal of Petrology*, **29**, 445–522.

Black, P. M., Brothers, R. N. & Yokoyama, K., 1988. Mineral parageneses in eclogite-facies metadacites in northern New Caledonia. In: *Eclogites and Eclogite-Facies Rocks* (ed. Smith, D. C.), pp. 271–289. Elsevier.

van Blanckenburg, F., Villa, I. M., Baur, H., Morteani, G. & Steiger, R. H., 1989. Time calibration of a PT-path from the Western Tauern window, Eastern Alps: problem of closure temperature. *Contributions to Mineralogy and Petrology*, **101**, 1–11.

Çoğulu, E., 1967. Etude petrographique de la region de Mihaliççık. *Schweizerische Mineralogisch und Petrographische Mitteilungen*, **47**, 683–824.

Çoğulu, E. & Krummenacher, D., 1967. Problemes geochronometriques dans la partie NW de l'Anatolie Centrale (Turquie). *Schweizerische Mineralogisch und Petrographische Mitteilungen,* **47,** 825–833.

Compagnoni, R., 1977. The Sesia-Lanzo Zone: high pressure–low temperature metamorphism in the Austroalpine continental margin. *Rendiconti Societa Italiana di Mineralogia e Petrologia,* **33,** 335–374.

El-Shazly, A. K. & Liou, J. G., 1991. Glaucophane chloritoid-bearing assemblages from NE Oman: petrologic significance and a petrogenetic grid for high P metapelites. *Contributions to Mineralogy and Petrology,* **107,** 180–201.

Ernst, G., 1965. Mineral parageneses in Franciscan metamorphic rocks, Panoche Pass, California. *Geological Society of America Bulletin,* **76,** 879–914.

Evans, W. E., 1990. Phase relations of epidote-blueschists. *Lithos,* **25,** 3–23.

Guiraud, M., Holland, T. & Powell, R., 1990. Calculated mineral equilibria in the greenschist-blueschist-eclogite facies in Na_2O–FeO–MgO–Al_2O_3–SiO_2–H_2O. *Contributions to Mineralogy and Petrology,* **104,** 85–98.

Harris, N. B. W., Kelley, S. & Okay, A. I., 1994. Post-collisional magmatism and tectonics in northwest Anatolia. *Contributions to Mineralogy and Petrology,* in press.

Holland, T. J. B. & Powell, R., 1990. An enlarged and updated internally consistent thermodynamic dataset with uncertainties and correlations: the system K_2O–Na_2O–CaO–MgO–MnO–FeO–Fe_2O_3–Al_2O_3–TiO_2–SiO_2–C–H_2O–O_2. *Journal of Metamorphic Geology,* **8,** 89–124.

Jayko, A. S., Blake, M. C. & Harms, T., 1987. Attenuation of the Coast Range Ophiolite by extensional faulting, and nature of the Coast Range "Thrust", California. *Tectonics,* **4,** 475–488.

Kulaksız, S., 1981. Geology of the region of northwest of Sivrihisar (in Turkish). *Yerbilimleri,* **8,** 103–124.

Maluski, H., Bonneau, M. & Kienast, J. R., 1987. Dating the metamorphic events in the Cycladic area: $^{39}Ar/^{40}Ar$ data from metamorphic rocks of Syros (Greece). *Bulletin Societe Geologique France,* **8,** 833–842.

Massonne, H-J. & Schreyer, W., 1987. Phengite geobarometry based on the limiting assemblage with K-feldspar, phlogopite, and quartz. *Contributions to Mineralogy and Petrology,* **96,** 212–224.

McKee, B., 1962. Widespread occurrence of jadeite, lawsonite and glaucophane in central California. *American Journal of Science,* **260,** 596–610.

Monod, O., Andrieux, J. & Gautier, J., 1991. Pontides-Taurides relationships in the region of Eskişehir (NW Turkey). In: *Special Issue on Tectonics* (ed. Dewey, J. F.), *Bulletin of the Technical University of Istanbul,* **44,** 257–277.

Moore, D. E. & Liou, J. G., 1979. Mineral chemistry of some Franciscan blueschist facies metasedimentary rocks from the Diablo Range, California. *Geological Society of America Bulletin.,* **90,** 1089–1091.

Newton, R. C. & Haselton, H. T., 1981. Thermodynamics of the garnet–plagioclase–Al_2SiO_5–quartz geobarometer. In: *Thermodynamics of Minerals and Melts* (eds Newton, R. C., Navrotsky, A. & Wood, B. J.), pp. 129–145. Springer, New York.

Okay, A. I., 1980a. Mineralogy, petrology and phase relations of glaucophane-lawsonite zone blueschists from the Tavşanlı region, northwest Turkey. *Contributions to Mineralogy and Petrology,* **72,** 243–255.

Okay, A. I., 1980b. Lawsonite zone blueschists and a sodic amphibole producing reaction in the Tavşanlı region, northwest Turkey. *Contributions to Mineralogy and Petrology,* **75,** 179–186.

Okay, A. I., 1982. Incipient blueschist metamorphism and metasomatism in the Tavşanlı region, northwest Turkey. *Contributions to Mineralogy and Petrology,* **79,** 361–367.

Okay, A. I., 1984. Distribution and characteristics of the northwest Turkish blueschists. In: *The Geological Evolution of the Eastern Mediterranean* (eds Robertson, A. H. F. & Dixon, J. E.), *Geological Society of London Special Publication,* **17,** 455–466.

Okay, A. I., 1986. High-pressure/low-temperature metamorphic rocks of Turkey. In: *Blueschists and Eclogites* (eds Evans, B. W. & Brown, E. H.), *Geological Society of America Memoir,* **164,** 333–347.

Okrusch, M. & Bröcker, M., 1990. Eclogites associated with high-grade blueschists in the Cyclades archipelago, Greece: a review. *European Journal of Mineralogy,* **2,** 451–478.

Okrusch, M., Seidel, E. & Davis, E. N., 1978. The assemblage jadeite–quartz in the glaucophane rocks of Sifnos (Cyclades archipelago, Greece). *Neues Jahrbuch Mineralogische Abhandlungen,* **132,** 284–308.

Peacock, S. M., 1992, Blueschist-facies metamorphism, shear heating, and P-T-t paths in subduction shear zones. *Journal of Geophysical Research,* **97,** 16 793–17 707.

Pettijohn, E. J., 1975. *Sedimentary Rocks.* Harper & Row, Singapore.

Platt, J. P., 1986. Dynamics of orogenic wedges and the uplift of high-pressure metamorphic rocks. *Geological Society of America Bulletin,* **97,** 1037–1053.

Ridley, J., 1984. The significance of deformation associated with blueschist facies metamorphism on the Aegean Island of Syros. In: *The Geological Evolution of the Eastern Mediterranean* (eds Robertson, A. H. F. & Dixon, J. E.), *Geological Society of London Special Publication,* **17,** 545–550.

Robbins, G. A., 1972. Radiogenic argon diffusion in muscovite under hydrothermal conditions. *Unpubl. MSc Thesis, Brown University.*

Samson, S. D. & Alexander, E. C. Jr., 1987. Calibration of the interlaboratory ^{40}Ar–^{39}Ar dating standard MMhb1. *Chemical Geology,* **66,** 27–34.

Satır, M. & Friedrichsen, H., 1986. The origin and evolution of the Menderes Massif, W-Turkey: a rubidium/strontium and oxygen isotope study. *Geologische Rundschau,* **75,** 703–714.

Schliestedt, M., 1986. Eclogite–blueschist relationships as evidenced by mineral equilibrium in the high pressure metabasic rocks of Sifnos (Cycladic Islands), Greece. *Journal of Petrology,* **27,** 1439–1459.

Schliestedt, M. & Okrusch, M., 1988. Meta-acidites and silicic metasediments related to eclogites and glaucophanites in northern Sifnos, Cycladic archipelago, Greece. In: *Eclogites and Eclogite-Facies Rocks* (ed. Smith, D. C.), pp. 291–334. Elsevier.

Şengör, A. M. C. & Yılmaz, Y., 1981. Tethyan evolution of Turkey: a plate tectonic approach. *Tectonophysics,* **75,** 181–241.

Shau, Y. H., Feather, M. E., Essene, E. J. & Peacor, D. R., 1991. Genesis and solvus relations of submicroscopically intergrown paragonite and phengite in a blueschist from northern California. *Contribution to Mineralogy and Petrology,* **106,** 367–378.

Sobolev, N. V., Dobretsov, N. L., Bakirov, A. B. & Shatsky, V. S., 1986. Eclogites from various types of metamorphic complexes in the USSR and the problems of their origin. In: *Blueschists and Ecologites* (eds Evans, B. W. & Brown, E. H.), *Geological Society of America Memoir,* **164,** 349–364.

Theye, T. & Seidel, E., 1991. Petrology of low-grade high-pressure metapelites from the External Hellenides (Crete, Peloponnese); a case study with attention to sodic minerals. *European Journal of mineralogy,* **3,** 343–366.

Wijbrans, J. R., Schliestedt, M. & York, D., 1990. Single grain argon laser probe dating of phengites from the blueschist to greenschist transition on Sifnos (Cyclades, Greece). *Contributions to Mineralogy and Petrology,* **104,** 582–593.

Wijbrans, J. R., van Wees, J. D., Stephenson, R. A. & Cloetingh, S. A. P. L., 1993. Pressure-temperature-time evolution of the high-pressure metamorphic complex of Sifnos, Greece. *Geology,* **21,** 443–446.

Received 6 July 1993; revision accepted 9 December 1993.